

FairGE: Fairness-Aware Graph Encoding in Incomplete Social Networks

Renqiang Luo
Jilin University
Changchun, China
lrenqiang@outlook.com

Jing Ren
RMIT University
Melbourne, Australia
jing.ren@ieee.org

Enyan Dai
HKUST
Guangzhou, China
enyandai@hkust-gz.edu.cn

Huafei Huang
Adelaide University
Adelaide, Australia
hhuafei@outlook.com

Ziqi Xu*
RMIT University
Melbourne, Australia
ziqi.xu@rmit.edu.au

Tao Tang
Zhejiang University of Technology
Hangzhou, China
tao.tang@ieee.org

Mingliang Hou
Jinan University & TAL Education
Group
Guangzhou, China
teemohold@outlook.com

Feng Xia
RMIT University
Melbourne, Australia
f.xia@ieee.org

CCS Concepts

- **Information systems** → **Social networks; Data mining**; •
- **Computing methodologies** → **Spectral methods**.

Keywords

Social Networks, Graph Learning, Graph Transformers, Fairness, Incomplete Data

ACM Reference Format:

Renqiang Luo, Huafei Huang, Tao Tang, Jing Ren, Ziqi Xu*, Mingliang Hou, Enyan Dai, and Feng Xia. 2026. FairGE: Fairness-Aware Graph Encoding in Incomplete Social Networks. In *Proceedings of The Web Conference 2026 (The ACM Web Conference '26)*. ACM, New York, NY, USA, 12 pages. <https://doi.org/XXXXXX.XXXXXXX>

1 Introduction

Graph Transformers (GTs) address common Graph Neural Networks (GNNs) challenges such as over-smoothing [47], over-squashing [17], and long-range dependencies [6] by employing global attention to capture long-range node interactions [38, 43]. Despite these advantages, GTs often overlook inherent biases in graph data, leading to discriminatory predictions towards sensitive subgroups (e.g., gender and race) [31]. This issue is particularly critical in social networks, where fairness directly affects user trust and system reliability [3, 46]. Here, algorithmic fairness requires that model predictions remain unbiased with respect to sensitive attributes (e.g., gender, race, region, and other potential factors), ensuring equitable treatment of diverse subgroups [14]. The challenge is further compounded by the frequent absence of sensitive attributes, as individuals are often unwilling or unable to disclose such information due to privacy and ethical concerns [9]. Therefore, addressing fairness under incomplete sensitive attributes is essential for real-world social network applications, where reliable and equitable outcomes must be guaranteed [45].

When under the incomplete social networks (i.e., sensitive attributes are partially missing), the fairness performance of existing fairness-aware methods often deteriorates. As shown in Figure 1,

* Corresponding Author.

Permission to make digital or hard copies of all or part of this work for personal or classroom use is granted without fee provided that copies are not made or distributed for profit or commercial advantage and that copies bear this notice and the full citation on the first page. Copyrights for components of this work owned by others than the author(s) must be honored. Abstracting with credit is permitted. To copy otherwise, or republish, to post on servers or to redistribute to lists, requires prior specific permission and/or a fee. Request permissions from permissions@acm.org.

The ACM Web Conference '26, Dubai, United Arab Emirates

© 2026 Copyright held by the owner/author(s). Publication rights licensed to ACM.
ACM ISBN 978-1-4503-XXXX-X/2018/06
<https://doi.org/XXXXXX.XXXXXXX>

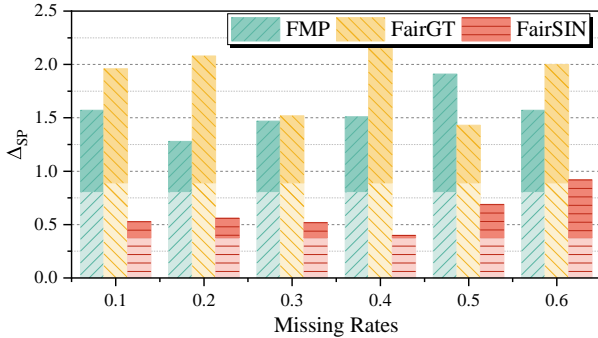


Figure 1: Impact of different missing rates of sensitive attributes on fairness-aware methods (FMP [21], FairGT [31], and FairSIN [42]) on the Credit dataset [20]. Δ_{SP} is reported as the fairness metric (see Section 3.2), where higher values indicate lower fairness. Lighter bars correspond to results on complete data, while darker bars indicate the additional increase due to missing attributes. For instance, in FMP, Δ_{SP} is about 0.78 with complete data but increases to around 1.6 at a missing rate of 0.1.

fairness degradation does not increase monotonically with the missing rate; rather, the presence of missing attributes triggers deterioration, whose severity depends on how current methods address incompleteness. For instance, FMP [21] and FairSIN [42] rely on attribute imputation, while FairGT [31] assumes complete sensitive attributes. Both strategies leave model outputs correlated with sensitive information, creating privacy risks, as prior work has shown that such correlations can be exploited to reconstruct private attributes [2, 16]. Therefore, developing fairness-aware GTs that ensure fairness without depending on attribute generation or complete attribute disclosure remains an urgent challenge.

A key challenge for GTs is to effectively encode both node and structural information, which can be addressed through multi-hop aggregation. This study applies spectral theory to analyse algorithmic fairness under incomplete attributes. Fairness is quantified by the similarity between the learned representation and the original sensitive attribute distribution [30]. Our analysis shows that leveraging the largest eigenvalues and corresponding eigenvectors effectively encodes node and structural information, thereby capturing multi-hop neighbourhood signals. Spectral truncation also preserves similarity to the original sensitive attribute distribution, even with incomplete data. Moreover, padding missing sensitive attributes with zeros maintains consistency with the complete-data scenario while avoiding attribute reconstruction.

Building on this analysis, we propose **FairGE** (Fair Graph Encoding), a fairness-aware approach for GTs in incomplete social networks. FairGE is built on two core principles: (i) preserving fairness by selecting principal spectral components, and (ii) maintaining the independence of sensitive attributes through zero-padding. Concretely, FairGE first handles incomplete attributes by padding them with zeros, thereby approximating the original attribute distribution during encoding. It then computes the m largest eigenvalues and their corresponding eigenvectors of the adjacency matrix, where spectral truncation captures multi-hop interactions while reducing the influence of non-principal components. The resulting encoding

is integrated into GTs to produce fair node representations without reconstructing sensitive attributes.

The contributions are summarised as follows:

- We propose FairGE, a novel fairness-aware framework for GTs on incomplete social networks. By avoiding attribute generation, FairGE mitigates privacy risks and ethical concerns linked to sensitive information restoration.
- We establish a theoretical foundation showing that FairGE encodes both node attributes and structural information under incompleteness. Through spectral truncation and zero-padding, it ensures fairness without reconstructing sensitive data.
- Extensive experiments on seven real-world social network datasets show that FairGE consistently improves fairness, yielding over 16% gains in both statistical parity and equality of opportunity compared with state-of-the-art methods.

2 Related Work

2.1 Graph Transformers

GTs have demonstrated strong potential in graph representation learning by providing global receptive fields [28, 33, 44]. Models such as GraphTrans [39] and SAN [25] strengthen long-range dependency modelling through attention mechanisms and spectral encodings. NAGphormer [7] extends this paradigm by treating nodes as sequences of token vectors and leveraging selected Laplacian eigenvectors to encode structural topology and enable multi-hop message aggregation. These developments have positioned Transformer-based graph models at the core of a wide range of social network applications requiring expressive, non-local reasoning.

Despite these advances, fairness remains insufficiently addressed in GTs. Most existing models either overlook or amplify biases embedded in graph data due to absence of explicit fairness-aware mechanisms. Although FairGT [31] marks an initial step by leveraging high-eigenvalue spectral attributes to promote equitable representations, its reliance on complete access to sensitive attributes limits practical deployment. In social networks, where sensitive information (e.g., demographic attributes or regional identifiers) is often noisy, incomplete, or unavailable, this limitation becomes particularly restrictive. This underscores the need for fairness-aware GTs that are robust to incomplete sensitive attributes, enabling equitable representation learning in real-world social network applications.

2.2 Fairness-aware GNNs in Incomplete Social Networks

Fairness-aware GNNs have attracted growing attention, with methods designed to protect or regulate sensitive attributes during learning [13]. Representative models like FairGB [27] and FUGNN [30] employ group balancing, counterfactual mixup, and spectral regularisation to jointly optimise fairness and utility. However, most of these approaches assume full access to sensitive attributes, which is often unrealistic in social network applications where such information is incomplete due to privacy constraints [8, 11].

To address this challenge, recent approaches such as FairGNN [10] and FairAC [18] integrate attribute estimation and debiasing strategies under incomplete sensitive attributes. However, these methods

rely on generating or inferring sensitive attributes, which can reintroduce privacy risks by reconstructing deliberately withheld data. Furthermore, most fairness-aware designs are tightly coupled with GNN-specific operations, limiting their applicability to GTs, that encode structure differently and capture global dependencies [40?]. Consequently, enabling fairness-aware GTs in incomplete social networks remains a critical yet underexplored challenge.

3 Preliminaries

3.1 Notations

Unless otherwise specified, the following notation is used throughout this study: sets are denoted by copperplate uppercase letters (e.g., \mathcal{A}), matrices by bold uppercase letters (e.g., \mathbf{A}), and vectors by bold lowercase letters (e.g., \mathbf{x}). The social network is denoted as a graph, which is represented as $\mathcal{G} = (\mathcal{V}, \mathbf{A}, \mathbf{H})$, where \mathcal{V} is the set of n nodes, $\mathbf{A} \in \mathbb{R}^{n \times n}$ is the adjacency matrix, and $\mathbf{H} \in \mathbb{R}^{n \times d}$ is the node attribute matrix with d denoting attribute dimension.

The spectrum of \mathbf{A} reflects the graph's structural topology [4]. Since \mathbf{A} is symmetric, its eigendecomposition can be written as $\mathbf{A} = \mathbf{P}\Lambda\mathbf{P}^\top$, where $\mathbf{P} = (\mathbf{p}_1, \mathbf{p}_2, \dots, \mathbf{p}_n)$ with $\mathbf{p}_i \in \mathbb{R}^{n \times 1}$. The diagonal matrix $\Lambda = \text{diag}(\lambda_1, \lambda_2, \dots, \lambda_n)$ contains the eigenvalues of \mathbf{A} , ordered such that $|\lambda_1| > |\lambda_2| \geq \dots \geq |\lambda_n|$. Here, \mathbf{p}_i corresponds to λ_i , where \mathbf{p}_1 is associated with the dominant eigenvalue $|\lambda_1|$.

This indexing rules follow those of NumPy in Python. For a matrix \mathbf{A} , $\mathbf{A}[i, j]$ denotes the entry at the i -th row and the j -th column, while $\mathbf{A}[i, :]$ and $\mathbf{A}[:, j]$ denote the i -th row and j -th column, respectively. In social networks, many attributes are typically withheld by users and are therefore regarded as sensitive attributes [32]. For the attribute matrix \mathbf{H} , each column corresponds to one sensitive attribute, denoted by $\mathbf{H}[:, s]$. For binary sensitive attributes, the entries take values $\mathbf{H}[i, s] \in \{0, 1\}$. When sensitive attributes are incomplete, they denote as $\mathbf{H}'[:, s]$, and $\mathbf{H}'[:, s](0)$ denotes padding zeros for incomplete sensitive attributes.

3.2 Fairness Evaluation Metrics

Fairness in binary classification is considered with predicted labels $\hat{y} \in \{0, 1\}$, ground truth labels $y \in \{0, 1\}$, and a binary sensitive attribute $s \in \{0, 1\}$. Both metrics are commonly used to assess fairness on the test set.

Statistical Parity [15] measures the difference in positive prediction rates between sensitive groups:

$$\Delta_{\text{SP}} = |\mathbb{P}(\hat{y} = 1 \mid \mathbf{H}[i : s] = 0) - \mathbb{P}(\hat{y} = 1 \mid \mathbf{H}[i : s] = 1)|. \quad (1)$$

Equal Opportunity [19] evaluates the gap in true positive rates across sensitive groups:

$$\Delta_{\text{EO}} = |\mathbb{P}(\hat{y} = 1 \mid y = 1, \mathbf{H}[i : s] = 0) - \mathbb{P}(\hat{y} = 1 \mid y = 1, \mathbf{H}[i : s] = 1)|. \quad (2)$$

3.3 Transformer

The Transformer architecture comprises multiple layers, each with a self-attention module and a position-wise feed-forward network (FFN). Let $\mathbf{X} = [h_1^\top, \dots, h_j^\top]^\top \in \mathbb{R}^{i \times d_m}$ denote the input to the self-attention module, where d_m is the hidden dimension, and $h_j \in \mathbb{R}^{1 \times d_m}$ is the hidden representation at position j . The input matrix \mathbf{X} is projected using three weight matrices: $W_Q \in \mathbb{R}^{d_m \times d_K}$ (query),

$W_K \in \mathbb{R}^{d_m \times d_K}$ (key), and $W_V \in \mathbb{R}^{d_m \times d_V}$ (value). The self-attention mechanism is computed as follows:

$$Q = \mathbf{X}W_Q, \quad K = \mathbf{X}W_K, \quad V = \mathbf{X}W_V, \quad \text{Attn}(\mathbf{X}) = \text{Softmax}\left(\frac{QK^\top}{\sqrt{d_K}}\right)V. \quad (3)$$

For simplicity, it is assumed $d_K = d_V$, focusing on the self-attention module. Extending this to multi-head attention is straightforward, and bias terms are omitted for clarity.

4 Theoretical Discovery

Algorithmic fairness is quantified by measuring the similarity between the inferred and the original distributions of sensitive attributes, which aligns with the principle of sensitive attribute independence. A graph representation that preserves this similarity, even under incomplete attributes and without resorting to feature generation, can thus promote fairness in scenarios where sensitive attributes are missing.

We analyse the effect of structural encodings, particularly the adjacency matrix and its spectral truncation, on fairness preservation. Our results show that using only principal eigenvectors preserves the independence of sensitive attributes, even in incomplete social networks. Moreover, combining zero-padding with spectral truncation restores the original sensitive attribute distribution without relying on synthetic data, ensuring fairness in graph representation. Detailed proofs are provided in Appendix B.

4.1 Spectral Truncation as Structural Topology Encoding

For complete sensitive attributes, prior work has demonstrated that the principal eigenvectors significantly influence the similarity between the distribution of original sensitive attributes and that of their multi-hop propagations:

Lemma 1 [31]: *The similarity between the distribution of original sensitive attributes and that of multi-hop sensitive attributes exhibits a strong correlation with the principle eigenvectors.*

$$\lim_{k \rightarrow \infty} \cos(\langle \mathbf{A}^k \mathbf{H}[:, s], \mathbf{H}[:, s] \rangle) = \cos(\langle \mathbf{p}_1, \mathbf{H}[:, s] \rangle). \quad (4)$$

Building upon this observation, this study further investigates the case with incomplete sensitive attributes $\mathbf{H}'[:, s]$.

Theorem 1: *The effect of utilising the principal eigenvector as a structural encoding, in comparison to using multiple adjacency matrices as structural topology encoding for multi-hop sensitive attributes under incomplete sensitive attributes, can be approximated. The following equation holds:*

$$\lim_{k \rightarrow \infty} \cos(\langle \mathbf{A}^k \mathbf{H}'[:, s], \mathbf{H}'[:, s] \rangle) = \cos(\langle \mathbf{p}_1, \mathbf{H}'[:, s] \rangle). \quad (5)$$

Theorem 1.1: *In cases where multiple maximal eigenvalues exist, the conclusions remain analogous, with further elaboration as following:*

$$\lim_{k \rightarrow \infty} \cos(\langle \mathbf{A}^k \mathbf{H}'[:, s], \mathbf{H}'[:, s] \rangle) \geq \frac{1}{\sqrt{j}} \sum_{i=1}^j \cos(\langle \mathbf{H}'[:, s], \mathbf{p}_i \rangle). \quad (6)$$

Theorem 1.2: *The effect of non-principal eigenvalues diminishes at an exponential rate.*

The presence of a large spectral gap ensures that the principal eigenvectors dominate even in shallow architectures with finite depth (e.g., $k = 2$ or 3), enabling spectral truncation to effectively encode multi-hop structural information. Importantly, this property guarantees that the conclusions remain valid even when GTs operate under limited depth, a setting commonly adopted in practice. Moreover, by avoiding entanglement between incomplete sensitive attributes and structural encodings, this approach preserves algorithmic fairness while simultaneously enhancing the expressiveness of graph representations. These insights motivate the design choice of focusing on the dominant spectrum and excluding non-principal eigenvectors for fair and informative structural encoding.

Theorem 2: *When sensitive attributes incomplete in social networks, utilising principal eigenvectors as structural topology encoding can effectively reproduce the representation results with the adjacency matrix under complete attributes. The following equation holds:*

$$\lim_{k \rightarrow \infty} \cos(\langle \mathbf{A}^k \mathbf{H}[:, s], \mathbf{H}'[:, s] \rangle) = \cos(\langle \mathbf{p}_1, \mathbf{H}'[:, s] \rangle). \quad (7)$$

The spectral truncation ensures that the encoded graph structure remains robust even under finite-depth architectures, enabling accurate representation of multi-hop structural information. At the same time, it preserves fairness by avoiding the generation or reconstruction of incomplete sensitive attributes, thereby mitigating privacy risks while maintaining expressive graph encodings.

4.2 Combining Padding Zeros and Spectral Truncation

Theorem 3: *Padding incomplete value with zeros can effectively recover the neighbouring sensitive attribute information with incomplete sensitive attributes. The following equation holds:*

$$\begin{aligned} \lim_{k \rightarrow \infty} \cos(\langle \mathbf{A}^k \mathbf{H}'[:, s](0), \mathbf{H}[:, s] \rangle) \\ = \lim_{k \rightarrow \infty} \cos(\langle \mathbf{A}^k \mathbf{H}[:, s], \mathbf{H}[:, s] \rangle). \end{aligned} \quad (8)$$

In addition, the padding value 0 does not represent a fixed property; rather, it aligns with our design principle of avoiding synthetic data generation. By analogy to **Theorem 1.2**, a similar phenomenon holds for incomplete sensitive attributes. Even with a limited number of layers ($k = 2$ or 3), this conclusion remains valid due to the significant spectral gap in real-world datasets ($\lambda_1 \gg \lambda_2$), ensuring the dominance of the principal eigenvector in the multi-hop propagation. This theorem is valid if female is 0 or male is 0. In summary, under the scenario of incomplete social networks, the sensitive attributes of multi-hop neighbour information are predominantly influenced by the eigenvector corresponding to the largest magnitude eigenvalue (or multiple eigenvectors associated with the largest magnitude eigenvalue). In addition in cases where sensitive attributes are incomplete, padding the incomplete attributes with zeros enhances the fairness and utility of these principal eigenvectors in the model. Therefore, in the context of incomplete social networks, this study proposes that combining spectral truncation with simple zero-padding significantly improves fairness.

5 Design of FairGE

FairGE for fairness-aware node classification in GTs integrates three key components. First, zero padding addresses incomplete

sensitive attributes, mitigating privacy risks while, as shown in our theoretical analysis, preserving multi-hop neighbour information and sensitive attribute independence. Second, spectral truncation leverages principal eigenvectors to reconstruct multi-hop signals, improving both fairness and accuracy. Finally, the combined encoding from zero padding and spectral truncation is integrated into the GT, enabling efficient and fair node classification. Figure 2 illustrates the model architecture.

5.1 Padding incomplete Sensitive attributes

In graph mining tasks, node attribute information is crucial. To address incomplete sensitive attributes, FairGE proposes a zero-padding encoding. This method captures multi-hop information that mirrors original sensitive attribute patterns.

For a given node v , its k -hop neighbourhood is denoted as $\mathcal{V}^{(k)}$, with $\mathcal{V}^{(0)} = \{v\}$ representing the node itself. In GTs with incomplete attributes, the k -hop neighbourhood information is transformed into an attribute embedding $\mathbf{H}'_v^{(k)}$ via an aggregation operator Φ , which integrates information from nodes across multiple hop distances. Formally, the aggregation for node v is defined as:

$$\mathbf{H}'_v^{(k)} = \Phi(v, \mathcal{V}^{(1)}, \dots, \mathcal{V}^{(k)}). \quad (9)$$

Using this formulation, FairGE computes the multi-hop attribute information for any node. To simplify the node attribute encoding, FairGE decomposes the sequence $\mathbf{S} = (\mathbf{H}'^{(0)}, \mathbf{H}'^{(1)}, \dots, \mathbf{H}'^{(k)})$, where $\mathbf{H}'^{(k)} \in \mathbb{R}^{n \times d}$ denotes the multi-hop attribute matrix and $\mathbf{H}'^{(0)}$ corresponds to the original attribute matrix. Given adjacency matrix \mathbf{A} of \mathcal{G} , the multi-hop attribute matrix is computed as:

$$\mathbf{H}'^{(k)} = \mathbf{A}^k \mathbf{H}'. \quad (10)$$

As shown in **Theorem 3** (see Equation (8)), the zero-padding encoding $\mathbf{H}'^{(0)}$ closely resembles the original sensitive attribute structure. Encoding multi-hop information using zero-padding helps capture the correlations across hops and contributes significantly to fairness in GTs.

5.2 Restoring Multi-hop Neighbour Information

Beyond node attribute encoding, structural topology encoding is also crucial for capturing valuable graph information. To restore multi-hop neighbour information, FairGE introduces a novel structural topology encoding, which utilises spectral truncation to process multi-hop information. Spectral graph theory reveals that algebraic connectivity (the second smallest eigenvalue) and spectral radius (the largest eigenvalue) are deeply connected to the geometric properties of the graph [25].

Drawing from **Theorem 1** and **Theorem 2**, FairGE adopts spectral truncation (ST) of the adjacency matrix to recover the incomplete sensitive information of multi-hop neighbours. Specifically, FairGE selects the eigenvectors \mathbf{P}_{ST} corresponding to the m largest eigenvalues \mathbf{e}_{ST} , as follows:

$$\mathbf{e}_{\text{ST}} = (\lambda_1, \lambda_2, \dots, \lambda_m), \quad \mathbf{P}_{\text{ST}} = (\mathbf{p}_1, \mathbf{p}_2, \dots, \mathbf{p}_m). \quad (11)$$

In FairGE, the hyperparameter m dictates the number of principal eigenvectors retained from the graph spectrum. To compute these efficiently, FairGE uses the Arnoldi Package [5] for its high computational efficiency and accuracy. While full eigendecomposition typically has a cubic time complexity $O(n^3)$, this package

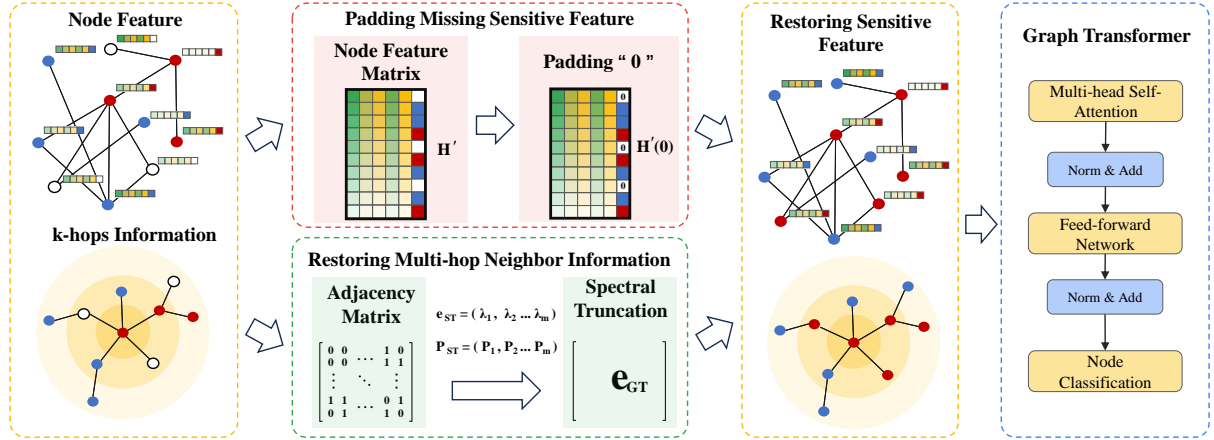


Figure 2: The illustration of FairGE. For graphs containing two sensitive attributes (represented as red and blue) alongside incomplete sensitive attributes (white), FairGE effectively restores and preserves the original sensitive attributes while also capturing multi-hop neighbour information.

reduces FairGE’s complexity to $O(nm^2)$ in time and $O(n)$ in space. Even with small values of m , FairGE remains highly effective with minimal performance fluctuations.

5.3 FairGE for Node Classification

In the FairGE framework, the process begins by concatenating a matrix derived from the adjacency matrix’s eigendecomposition to encode the structural topology, as defined by Equation (11). To address incomplete sensitive attributes, FairGE then applies zero padding, denoted as $H'(0)$.

Next, FairGE applies a position encoding to the eigenvalues using the following sinusoidal and cosine functions:

$$\begin{aligned} \rho(\lambda_{2i}) &= \sin(\lambda_{2i}/10000^{2i/d}), \\ \rho(\lambda_{2i+1}) &= \cos(\lambda_{2i+1}/10000^{2i/d}), \end{aligned} \quad (12)$$

resulting in a position-encoded (PE) eigenvalue sequence:

$$e_{PE} = (\rho(\lambda_1), \rho(\lambda_2), \dots, \rho(\lambda_m)). \quad (13)$$

FairGE then projects this transformed sequence, which encodes the structural topology, into the Transformer architecture [35]. The Transformer consists of multi-head self-attention (MHA) and a position-wise feed-forward network (FFN), with Layer Normalization (LN) applied before each block. The FFN is composed of two linear layers with a GELU activation function:

$$\begin{aligned} e_{MHA} &= MHA(LN(e_{PE})) + e_{PE}, \\ e_{GT} &= FFN(LN(e_{MHA})) + e_{MHA}. \end{aligned} \quad (14)$$

Finally, FairGE refines the spectral representation using the learned embedding e_{GT} and transforms the zero-padded attributes $H'(0)^{(l)}$ at each layer, where $W^{(l-1)}$ denotes the trainable transformation matrix of the $(l-1)$ -th layer and $\sigma(\cdot)$ is a non-linear activation function:

$$\begin{aligned} H_{\text{train}}^{(l)} &= P_{ST} \cdot (e_{GT} \odot P_{ST}^T H'(0)^{(l)}), \\ H^{(l)} &= \sigma((H^{(l-1)} || H_{\text{train}}^{(l-1)}) W^{(l-1)}). \end{aligned} \quad (15)$$

By stacking multiple GT layers, FairGE effectively learns node representations that incorporate graph information, improving the model’s performance even with incomplete sensitive attributes.

6 Experiments

6.1 Datasets

Node classification is adopted as the downstream task, employing seven real-world social network datasets: **Facebook** [26], **Income** [1], **Bail** [22], **Credit** [20], **Pokec-z** [34], **Pokec-n** [34], and **AMiner-S** [36]. These datasets cover diverse social contexts, including online friendship networks, financial and judicial social interactions, and academic collaboration. Notably, **AMiner-S** includes multi-class sensitive attributes, where sensitive attributes span more than two distinct categories (e.g., multiple regions instead of binary gender).

Table 1: Statistics of the seven real-world datasets.

Dataset	# Nodes	# Edges	Sensitive attribute	Label
Facebook	1,045	53,498	Gender	Education
Income	14,821	100,483	Race	Income
Bail	18,876	321,308	Race	Recidivism
Credit	30,000	137,377	Age	Default
Pokec-z	67,797	882,765	Region/Gender	Field
Pokec-n	66,569	729,129	Region/Gender	Field
AMiner-S	39,424	52,460	Affiliation	Field

To support fairness analysis across different types of sensitive attributes, the **Pokec** datasets are further divided into variants: **Pokec-z-R** and **Pokec-n-R** use living region as the sensitive attribute, while **Pokec-z-G** and **Pokec-n-G** use gender. For datasets with more than two ground-truth label classes, label 0 and 1 are reained, and all class greater than 1 are merged into class 1. The data is split into 25% for validation and 25% for testing. For training, 100 nodes are sampled from the **Facebook** dataset, 6,000 from **Credit**, and 1,000 from each of **Income**, **Bail**, **Pokec-z**, **Pokec-n**, and **AMiner-S**. This parameter setting follows prior work in fairness-aware graph learning [10, 30].

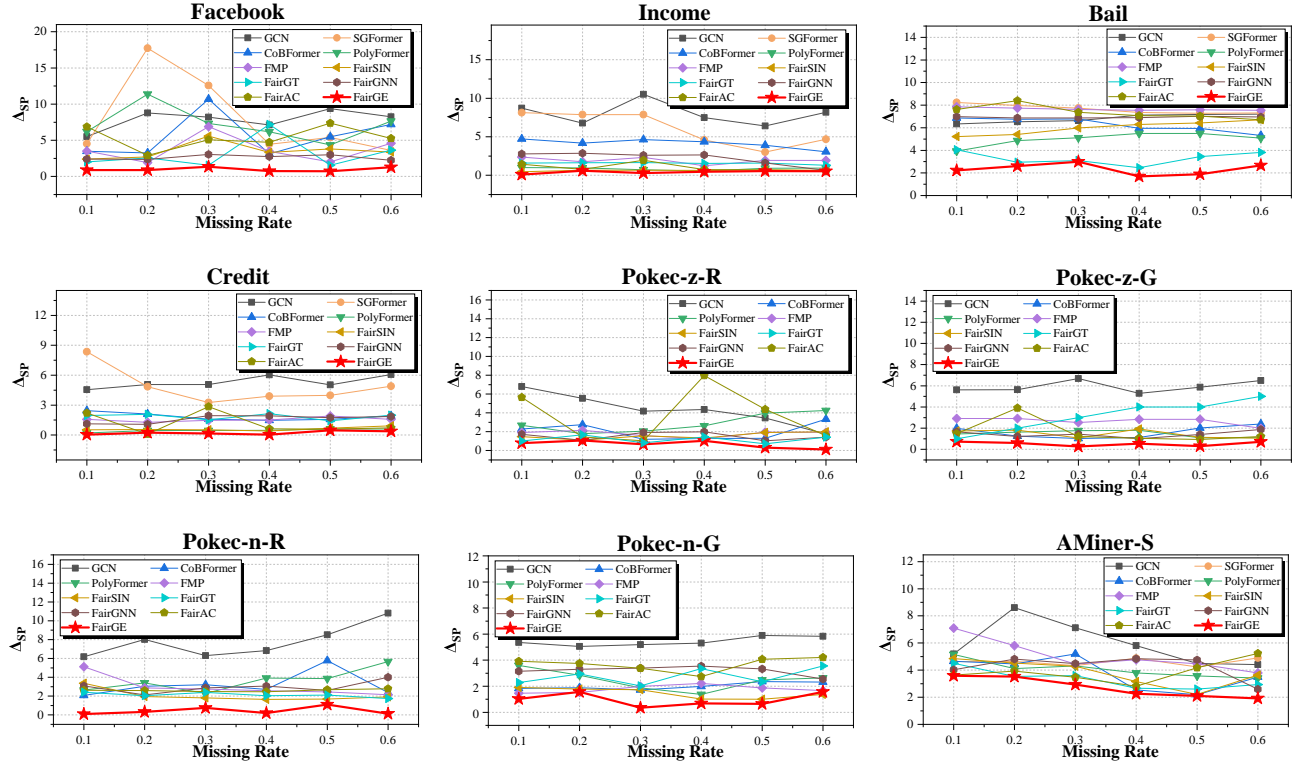
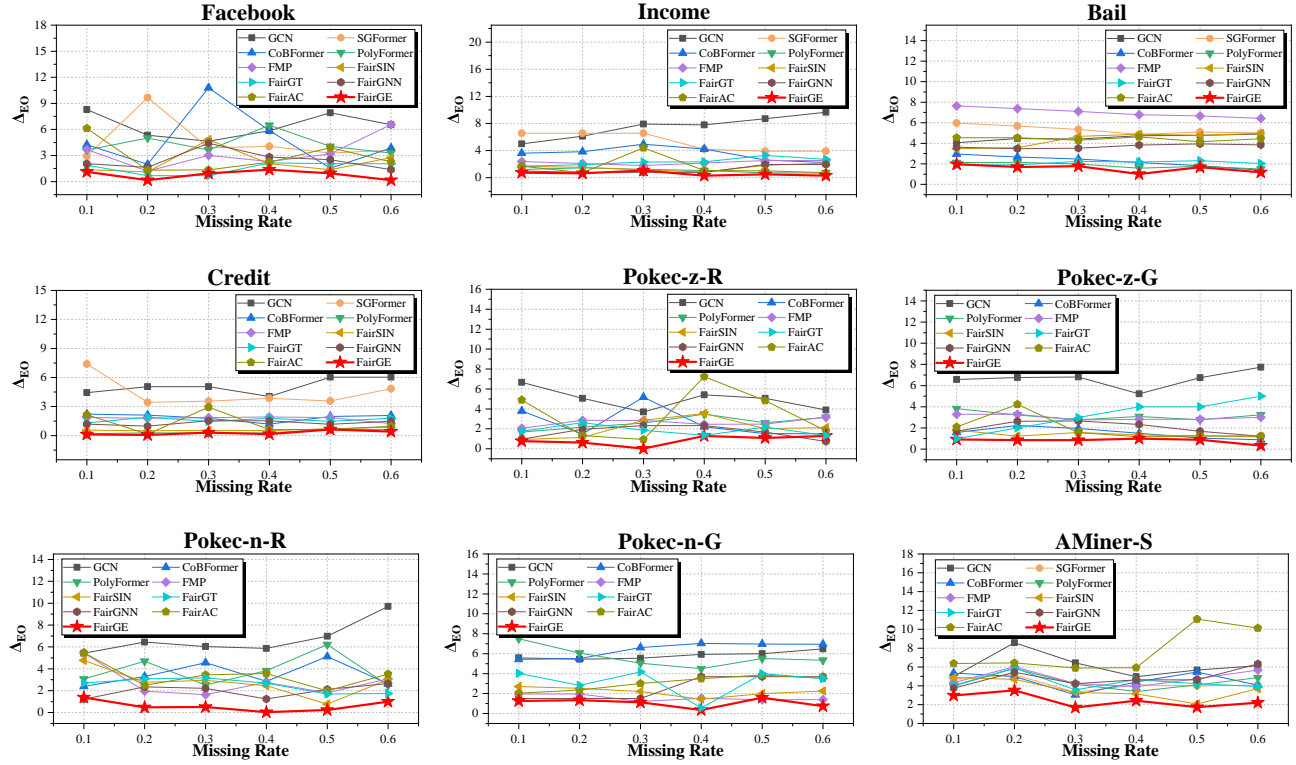
Figure 3: Comparison of Δ_{SP} between FairGE and baseline models.Figure 4: Comparison of Δ_{EO} between FairGE and baseline models.

Table 2: Comparison results of FairGE and baseline models on the Credit and AMiner-S datasets. Red numbers denote the best performance, and blue numbers denote the second best.

Missing Rate Metrics	Credit(0.1)			Credit(0.2)			Credit(0.3)		
	ACC(%) \uparrow	$\Delta_{SP}(\%)_{\downarrow}$	$\Delta_{EO}(\%)_{\downarrow}$	ACC(%) \uparrow	$\Delta_{SP}(\%)_{\downarrow}$	$\Delta_{EO}(\%)_{\downarrow}$	ACC(%) \uparrow	$\Delta_{SP}(\%)_{\downarrow}$	$\Delta_{EO}(\%)_{\downarrow}$
GCN	75.70 \pm 0.82	4.54 \pm 0.31	4.44 \pm 1.25	75.37 \pm 0.96	5.06 \pm 0.48	5.06 \pm 0.22	75.37 \pm 1.34	5.06 \pm 0.73	5.06 \pm 0.29
SGFormer	72.23 \pm 1.33	8.35 \pm 0.27	7.39 \pm 0.69	72.70 \pm 0.84	4.85 \pm 0.54	3.43 \pm 0.19	73.23 \pm 0.91	3.26 \pm 0.46	3.55 \pm 0.16
CoBFormer	75.67 \pm 0.95	2.44 \pm 0.39	2.22 \pm 1.18	75.39 \pm 0.73	2.11 \pm 0.49	2.11 \pm 0.25	76.01 \pm 1.02	1.59 \pm 0.59	1.78 \pm 0.24
Polynormer	77.24 \pm 1.08	<u>0.20 \pm 0.13</u>	<u>0.19 \pm 0.12</u>	76.99 \pm 0.58	0.46 \pm 0.37	0.28 \pm 0.26	76.21 \pm 1.17	<u>0.45 \pm 0.43</u>	<u>0.26 \pm 0.19</u>
FMP	75.96 \pm 1.21	1.57 \pm 0.42	1.87 \pm 1.36	76.00 \pm 0.65	1.28 \pm 0.50	1.78 \pm 0.33	76.11 \pm 1.29	1.47 \pm 0.61	1.85 \pm 0.28
FairSIN	<u>77.64 \pm 1.14</u>	0.53 \pm 0.23	0.57 \pm 0.77	77.72 \pm 0.68	0.56 \pm 0.46	0.49 \pm 0.21	77.50 \pm 1.32	0.52 \pm 0.50	0.54 \pm 0.32
FairGT	77.27 \pm 1.47	1.96 \pm 0.32	1.30 \pm 1.03	77.26 \pm 0.79	2.08 \pm 0.45	1.91 \pm 0.24	77.29 \pm 1.15	1.52 \pm 0.48	1.46 \pm 0.26
FairGNN	75.06 \pm 0.78	1.12 \pm 0.18	1.18 \pm 1.15	74.29 \pm 0.64	1.07 \pm 0.59	0.98 \pm 0.36	75.10 \pm 0.92	1.94 \pm 0.71	1.53 \pm 0.33
FairAC	77.18 \pm 1.03	2.21 \pm 0.26	2.15 \pm 0.87	<u>77.87 \pm 0.76</u>	<u>0.09 \pm 0.05</u>	<u>0.15 \pm 0.12</u>	<u>77.67 \pm 1.08</u>	2.84 \pm 0.54	2.93 \pm 0.28
FairGE	77.72 \pm 0.97	0.03 \pm 0.02	0.12 \pm 0.10	78.08 \pm 0.67	0.24 \pm 0.13	0.07 \pm 0.04	77.67 \pm 1.35	0.16 \pm 0.12	0.30 \pm 0.09
Missing Rate	Credit(0.4)			Credit(0.5)			Credit(0.6)		
	75.85 \pm 1.45	6.03 \pm 0.29	4.04 \pm 1.23	74.85 \pm 0.98	5.03 \pm 0.47	6.04 \pm 0.31	74.85 \pm 1.12	6.06 \pm 0.69	6.04 \pm 0.24
SGFormer	73.40 \pm 0.89	3.89 \pm 0.12	3.85 \pm 0.56	73.34 \pm 0.78	3.98 \pm 0.51	3.58 \pm 0.19	72.37 \pm 0.87	4.89 \pm 0.32	4.85 \pm 0.15
CoBFormer	76.08 \pm 1.02	1.47 \pm 0.34	1.18 \pm 0.78	75.92 \pm 0.67	1.58 \pm 0.45	1.97 \pm 0.21	76.30 \pm 0.99	1.91 \pm 0.53	2.08 \pm 0.12
Polynormer	76.18 \pm 1.23	0.48 \pm 0.34	<u>0.27 \pm 0.18</u>	76.61 \pm 0.67	0.61 \pm 0.56	<u>0.65 \pm 0.23</u>	<u>77.62 \pm 1.01</u>	<u>0.60 \pm 0.42</u>	<u>0.64 \pm 0.18</u>
FMP	75.59 \pm 0.99	1.51 \pm 0.23	1.92 \pm 1.45	75.55 \pm 0.87	1.91 \pm 0.34	1.86 \pm 0.67	75.48 \pm 0.56	1.57 \pm 0.78	1.23 \pm 0.21
FairSIN	77.32 \pm 1.11	<u>0.40 \pm 0.23</u>	0.51 \pm 0.24	<u>77.21 \pm 0.69</u>	0.69 \pm 0.45	0.70 \pm 0.21	77.33 \pm 1.23	0.92 \pm 0.57	0.88 \pm 0.31
FairGT	77.12 \pm 1.34	2.15 \pm 0.32	1.78 \pm 0.68	77.09 \pm 0.72	1.43 \pm 0.48	1.48 \pm 0.24	76.76 \pm 1.19	2.00 \pm 0.46	1.78 \pm 0.27
FairGNN	75.03 \pm 0.76	1.92 \pm 0.18	1.52 \pm 1.15	76.39 \pm 0.64	1.75 \pm 0.59	1.16 \pm 0.36	75.66 \pm 0.92	1.86 \pm 0.71	1.47 \pm 0.33
FairAC	<u>77.75 \pm 1.03</u>	0.62 \pm 0.26	0.62 \pm 0.87	<u>77.77 \pm 0.76</u>	<u>0.59 \pm 0.44</u>	<u>0.65 \pm 0.22</u>	77.56 \pm 1.08	0.72 \pm 0.54	0.96 \pm 0.28
FairGE	77.60 \pm 0.97	0.04 \pm 0.03	0.15 \pm 0.09	77.13 \pm 0.67	0.48 \pm 0.53	0.64 \pm 0.34	78.20 \pm 1.35	0.37 \pm 0.22	0.41 \pm 0.39
Missing Rate Metrics	AMiner-S(0.1)			AMiner-S(0.2)			AMiner-S(0.3)		
	ACC(%) \uparrow	$\Delta_{SP}(\%)_{\downarrow}$	$\Delta_{EO}(\%)_{\downarrow}$	ACC(%) \uparrow	$\Delta_{SP}(\%)_{\downarrow}$	$\Delta_{EO}(\%)_{\downarrow}$	ACC(%) \uparrow	$\Delta_{SP}(\%)_{\downarrow}$	$\Delta_{EO}(\%)_{\downarrow}$
GCN	88.85 \pm 1.09	5.19 \pm 2.63	4.98 \pm 1.34	83.72 \pm 1.96	8.61 \pm 2.09	8.58 \pm 2.12	83.13 \pm 1.32	7.12 \pm 1.16	6.43 \pm 1.09
SGFormer	89.54 \pm 0.07	4.63 \pm 0.69	4.75 \pm 0.25	88.30 \pm 0.08	4.64 \pm 0.05	5.18 \pm 1.61	87.88 \pm 0.18	4.33 \pm 0.06	3.31 \pm 0.53
CoBFormer	88.13 \pm 1.26	4.65 \pm 0.94	5.36 \pm 2.65	87.86 \pm 0.28	4.46 \pm 0.78	4.99 \pm 3.60	86.26 \pm 0.40	5.19 \pm 1.09	3.05 \pm 1.57
Polynormer	89.42 \pm 0.19	5.16 \pm 0.91	3.98 \pm 1.51	88.68 \pm 0.34	4.11 \pm 0.21	5.86 \pm 2.70	87.99 \pm 1.34	4.31 \pm 0.79	4.18 \pm 1.79
FMP	88.33 \pm 0.96	7.10 \pm 2.02	4.33 \pm 1.92	86.46 \pm 1.52	5.81 \pm 1.57	6.03 \pm 1.63	85.84 \pm 1.26	4.44 \pm 1.65	4.24 \pm 0.78
FairSIN	85.74 \pm 1.60	4.85 \pm 3.78	4.88 \pm 1.72	84.25 \pm 0.01	4.52 \pm 1.89	4.68 \pm 1.24	84.04 \pm 0.16	4.29 \pm 0.24	3.28 \pm 0.22
FairGT	89.05 \pm 1.00	4.51 \pm 0.60	4.05 \pm 0.89	87.25 \pm 1.11	3.54 \pm 0.23	5.88 \pm 1.90	86.59 \pm 0.42	3.60 \pm 0.63	3.57 \pm 1.95
FairGNN	86.00 \pm 1.05	4.03 \pm 1.63	3.75 \pm 2.86	87.59 \pm 1.81	4.81 \pm 2.39	5.44 \pm 2.37	86.62 \pm 1.11	4.48 \pm 0.65	4.23 \pm 1.26
FairAC	78.94 \pm 2.04	3.63 \pm 2.10	6.37 \pm 2.03	79.61 \pm 0.02	3.93 \pm 0.04	6.43 \pm 1.31	80.86 \pm 0.06	3.47 \pm 1.13	5.88 \pm 1.51
FairGE	89.12 \pm 1.34	3.59 \pm 0.28	2.97 \pm 0.37	88.33 \pm 2.03	3.52 \pm 1.05	3.52 \pm 1.06	87.01 \pm 1.01	2.94 \pm 0.49	1.69 \pm 0.54
Missing Rate	AMiner-S(0.4)			AMiner-S(0.5)			AMiner-S(0.6)		
	83.08 \pm 1.87	5.81 \pm 1.27	4.96 \pm 1.77	81.48 \pm 1.36	4.49 \pm 0.90	5.67 \pm 1.08	81.89 \pm 1.71	4.41 \pm 1.01	6.13 \pm 1.46
SGFormer	85.54 \pm 1.35	4.87 \pm 0.86	4.11 \pm 2.07	84.57 \pm 0.51	4.24 \pm 0.37	4.00 \pm 1.74	83.47 \pm 1.00	4.90 \pm 0.42	4.06 \pm 0.84
CoBFormer	84.84 \pm 1.29	2.54 \pm 0.33	4.40 \pm 0.64	83.32 \pm 2.58	2.19 \pm 0.19	5.46 \pm 2.29	84.18 \pm 0.30	3.49 \pm 0.14	4.07 \pm 3.97
Polynormer	85.04 \pm 2.48	3.79 \pm 2.01	3.40 \pm 1.49	85.14 \pm 1.94	3.57 \pm 1.69	4.11 \pm 1.91	83.17 \pm 0.09	3.41 \pm 0.14	4.87 \pm 0.75
FMP	85.42 \pm 1.25	4.76 \pm 0.17	3.90 \pm 0.17	84.23 \pm 1.65	4.47 \pm 1.16	4.76 \pm 0.78	85.50 \pm 1.32	3.80 \pm 0.62	5.68 \pm 0.69
FairSIN	82.15 \pm 0.07	3.16 \pm 0.04	3.15 \pm 0.04	80.06 \pm 0.29	2.21 \pm 0.31	2.07 \pm 0.05	79.91 \pm 0.80	3.63 \pm 2.32	3.69 \pm 3.46
FairGT	84.26 \pm 1.88	2.66 \pm 1.39	4.65 \pm 2.04	82.12 \pm 0.38	2.60 \pm 0.61	4.23 \pm 1.87	80.24 \pm 0.00	2.94 \pm 0.60	3.92 \pm 0.42
FairGNN	83.58 \pm 0.35	4.84 \pm 1.98	4.63 \pm 2.49	83.36 \pm 1.77	4.75 \pm 1.22	4.64 \pm 2.54	82.58 \pm 1.93	2.59 \pm 1.28	6.33 \pm 1.18
FairAC	81.44 \pm 0.25	2.81 \pm 0.35	5.92 \pm 1.40	81.44 \pm 1.61	4.18 \pm 1.91	11.09 \pm 2.01	81.93 \pm 0.74	5.23 \pm 2.95	10.14 \pm 2.74
FairGE	85.56 \pm 0.53	2.26 \pm 1.89	2.42 \pm 0.24	83.77 \pm 0.69	2.10 \pm 0.19	1.74 \pm 0.01	83.52 \pm 0.35	1.92 \pm 0.29	2.21 \pm 0.43

6.2 Baselines

To evaluate FairGE, the study includes a comprehensive set of baselines. These comprise one vanilla GNN, GCN [24], and three state-of-the-art GTs: SGFormer [37], CoBFormer [41], and Polynormer [12]. For fairness-aware models, the benchmark incorporates two fairness-aware GNNs, FMP [21] and FairSIN [42], alongside one fairness-aware GT, FairGT [31]. Additionally, two attribute-generation capable fairness-aware GNNs, FairGNN [10] and FairAC [18], are included for comparison. The experimental setting is shown in Appendix C.

6.3 Comparison Results

To simulate incomplete sensitive features, this study uniformly masks values in the complete sensitive attribute column. This methodology is consistently applied across all models to ensure fair

comparison, with both original and incomplete-data distributions explicitly defined in the experiments. Figure 3 and Figure 4 provides a detailed comparison of the fairness evaluation metrics between the proposed FairGE and several baseline models across seven social network datasets with varying missing rates. Specifically, comparison experiments are conducted with missing rates ranging from 10% to 60%, covering both sparse and dense incompleteness scenarios. The overall accuracy, along with two key fairness metrics, Δ_{SP} and Δ_{EO} , part of them are reported in Table 2, and others are shown in <https://anonymous.4open.science/r/FairGE-609E>.

The **AMiner-S** dataset contains multi-class sensitive attributes. While previous fairness evaluation metrics are formulated for binary scenarios, they can be readily extended to multi-class sensitive attribute setting, as demonstrated by previous work [29]. To ensure

Table 3: Ablation study on different missing rates on Facebook.

Missing Rate Metrics	Facebook(0.1)			Facebook(0.2)			Facebook(0.3)		
	ACC(%) \uparrow	$\Delta_{SP}(\%) \downarrow$	$\Delta_{EO}(\%) \downarrow$	ACC(%) \uparrow	$\Delta_{SP}(\%) \downarrow$	$\Delta_{EO}(\%) \downarrow$	ACC(%) \uparrow	$\Delta_{SP}(\%) \downarrow$	$\Delta_{EO}(\%) \downarrow$
FairGE	88.17 \pm 1.63	0.89 \pm 0.04	1.12 \pm 0.15	86.64 \pm 1.69	0.89 \pm 0.17	0.17 \pm 0.08	85.50 \pm 0.99	1.35 \pm 0.18	0.95 \pm 0.29
FairGE (1)	85.50 \pm 1.98	1.66 \pm 0.81	2.15 \pm 0.59	85.11 \pm 2.03	1.37 \pm 0.39	1.90 \pm 0.84	83.59 \pm 2.20	1.39 \pm 0.27	1.98 \pm 0.35
FairGE (Mean)	87.79 \pm 1.56	1.02 \pm 0.12	1.98 \pm 0.32	85.02 \pm 1.65	1.45 \pm 0.34	1.81 \pm 0.86	81.68 \pm 1.43	2.11 \pm 0.38	2.16 \pm 0.54
FairGE w/o ST	82.06 \pm 2.11	2.23 \pm 0.84	2.08 \pm 0.23	81.68 \pm 1.09	1.94 \pm 0.16	1.46 \pm 0.32	79.39 \pm 2.21	3.51 \pm 1.54	2.88 \pm 1.07

Missing Rate	Facebook(0.4)			Facebook(0.5)			Facebook(0.6)		
	ACC(%) \uparrow	$\Delta_{SP}(\%) \downarrow$	$\Delta_{EO}(\%) \downarrow$	ACC(%) \uparrow	$\Delta_{SP}(\%) \downarrow$	$\Delta_{EO}(\%) \downarrow$	ACC(%) \uparrow	$\Delta_{SP}(\%) \downarrow$	$\Delta_{EO}(\%) \downarrow$
FairGE	84.73 \pm 1.97	0.75 \pm 0.19	1.38 \pm 0.89	83.59 \pm 1.73	0.73 \pm 0.49	0.95 \pm 0.38	83.59 \pm 1.83	1.27 \pm 0.68	0.17 \pm 0.04
FairGE (1)	80.15 \pm 0.89	1.03 \pm 0.12	0.21 \pm 1.45	82.44 \pm 0.32	1.63 \pm 0.67	1.64 \pm 0.45	76.34 \pm 0.23	1.45 \pm 0.76	2.15 \pm 0.21
FairGE (Mean)	80.15 \pm 1.56	0.91 \pm 0.08	2.41 \pm 1.23	77.86 \pm 1.56	1.78 \pm 0.45	1.90 \pm 0.67	75.57 \pm 2.34	1.90 \pm 0.87	2.34 \pm 0.45
FairGE w/o ST	77.86 \pm 1.23	3.99 \pm 0.34	1.91 \pm 0.98	76.33 \pm 1.67	2.48 \pm 0.56	2.68 \pm 0.23	76.72 \pm 2.12	3.50 \pm 0.45	2.42 \pm 0.67

Table 4: Runtime (s) of GT-based baseline models across seven datasets. OOM indicates out-of-memory errors.

Dataset	FairGE	SGFormer	CoBFormer	Polynormer	FairGT
Facebook	12.96	12.99	17.19	14.74	13.53
Income	19.77	24.97	25.58	22.65	22.83
Bail	18.89	33.09	28.06	26.41	24.56
Credit	23.15	45.70	31.92	29.89	31.34
Pokec-z	18.94	OOM	39.01	34.13	39.16
Pokec-n	18.13	OOM	37.21	31.94	37.81
AMiner-S	15.69	OOM	22.42	18.91	29.98

fairness across all sensitive subgroups, we quantify the core principle using the variance between them. Specifically, the fairness evaluation metrics for multi-class sensitive attributes are defined as follows, where class number denotes m :

$$\begin{aligned} \Delta_{SP} &= \text{Var}_{i=1}^m (|\mathbb{P}(\hat{y} = 1|s = i)|), \\ \Delta_{EO} &= \text{Var}_{i=1}^m (|\mathbb{P}(\hat{y} = 1|y = 1, s = i)|), \end{aligned} \quad (16)$$

FairGE consistently achieves superior fairness in node classification, outperforming other GTs and fairness-aware GNNs, even those generating data, especially under high incomplete data rates, a challenge where other methods like FairGT struggle. Beyond its robust fairness, FairGE also maintains high accuracy across all seven social network datasets. This exceptional performance extends to handling multiple sensitive attributes simultaneously, as evidenced by experiments on multi-sensitive datasets (Pokec-z and Pokec-n), where FairGE not only enhances fairness for individual sensitive attributes but also maintains it consistently across multiple ones, solidifying its role as a comprehensive fairness-aware solution for GTs with incomplete sensitive attributes.

6.4 Ablation Study

An ablation study reveals the individual impact of these techniques on prediction fairness and accuracy. The study systematically removed each component; for instance, the version without spectral truncation **w/o ST** was compared against the full FairGE model. Results in Table 3 consistently show FairGE outperforming **w/o ST** across accuracy, statistical parity (Δ_{SP}), and equal opportunity (Δ_{EO}), emphasizing spectral truncation's crucial role in preserving key data characteristics and ensuring fair outcomes.

Furthermore, the study analyzed the impact of zero padding by comparing FairGE with variants using different imputation strategies: FairGE (1), which pads with '1', and FairGE (Mean), which

fills with attribute means. These comparisons aimed to understand how different incomplete attribute handling strategies affect model performance and fairness. The results confirmed that zero padding leads to significant improvements, as FairGE consistently achieved higher accuracy and lower fairness disparity (Δ_{SP} and Δ_{EO}) compared to these ablated versions. This reinforces the importance of zero padding in enhancing both fairness and accuracy. In summary, the ablation study underscores the essential roles of both spectral truncation and zero padding in improving the fairness and performance of GTs within FairGE.

6.5 Training Cost Comparison

FairGE employs spectral truncation for encoding, which offers efficiency advantages over standard GTs. To validate this, we compare its training time with various GT baselines. For fairness, all methods are standardised with 128 hidden dimensions, 1 layer, 1 attention head, and 500 training epochs. As shown in Table 4, FairGE achieves superior accuracy and fairness in node classification without additional computational cost. This demonstrates its scalability, making FairGE a robust and efficient framework for fairness-aware GTs.

7 Conclusion

This paper addresses fairness issues in incomplete social networks. The proposed framework, FairGE, introduces two key components: zero-padding to handle incomplete sensitive attributes and spectral truncation to preserve multi-hop neighbor information. These components operate together to mitigate bias and maintain the independence of sensitive attributes in incomplete social networks. The design of FairGE enables effective encoding of both node and structural information, even in the absence of sensitive data, while avoiding synthetic attribute generation and thereby alleviating privacy concerns. Theoretical analysis demonstrates that the combination of spectral truncation and zero-padding maximises fairness while preserving model utility. Extensive experiments on seven social network datasets demonstrate that FairGE significantly improves fairness compared with state-of-the-art models, achieving substantial gains in statistical parity and equality of opportunity. Despite these strong results, FairGE remains sensitive to parameter selection (e.g., the number of principal eigenvectors and the padding strategy), highlighting the need for further optimisation. Future work will aim to enhance efficiency, robustness, and applicability to a broader range of sensitive attribute settings.

References

- [1] Arthur Asuncion and David Newman. 2007. UCI machine learning repository.
- [2] Yang Bai, Gaojie Xing, Hongyan Wu, Zihong Rao, Chuan Ma, Shiping Wang, Xiaolei Liu, Yimin Zhou, Jiajia Tang, Kaijun Huang, et al. 2024. Backdoor Attack and Defense on Deep Learning: A Survey. *IEEE Transactions on Computational Social Systems* (2024).
- [3] Nolwenn Bernard and Krisztian Balog. 2025. A Systematic Review of Fairness, Accountability, Transparency, and Ethics in Information Retrieval. *ACM Computing Surveys* 57, 6 (2025), 1–29.
- [4] Deyu Bo, Xiao Wang, Yang Liu, Yuan Fang, Yawen Li, and Chuan Shi. 2023. A Survey on Spectral Graph Neural Networks. *arXiv preprint arXiv:2302.05631* (2023).
- [5] Yunfeng Cai, Guanhua Feng, and Peng Li. 2021. A Note on Sparse Generalized Eigenvalue Problem. In *Proceedings of the 35th International Conference on Neural Information Processing Systems*. 23036–23048.
- [6] Huiyuan Chen, Zhe Xu, Chin-chia Michael Yeh, Vivian Lai, Yan Zheng, Minghua Xu, and Hanghang Tong. 2024. Masked Graph Transformer for Large-Scale Recommendation. In *Proceedings of the 47th International ACM SIGIR Conference on Research and Development in Information Retrieval*. 2502–2506.
- [7] Jinsong Chen, Kaiyuan Gao, Gaichao Li, and Kun He. 2023. NAGphormer: A Tokenized Graph Transformer for Node Classification in Large Graphs. In *The 11th International Conference on Learning Representations*.
- [8] Wei Chen, Yiqing Wu, Zhao Zhang, Fuzhen Zhuang, Zhongshi He, Ruobing Xie, and Feng Xia. 2024. FairGap: Fairness-Aware Recommendation via Generating Counterfactual Graph. *ACM Transactions on Information Systems* 42, 4 (2024), 1–25.
- [9] Enyan Dai and Suhang Wang. 2021. Say No to the Discrimination: Learning Fair Graph Neural Networks with Limited Sensitive Attribute Information. In *Proceedings of the 14th ACM International Conference on Web Search and Data Mining*. 680–688.
- [10] Enyan Dai and Suhang Wang. 2023. Learning Fair Graph Neural Networks with Limited and Private Sensitive Attribute Information. *IEEE Transactions on Knowledge and Data Engineering* 35, 7 (2023), 7103–7117.
- [11] Enyan Dai, Tianxiang Zhao, Huaiseng Zhu, Junjie Xu, Zhimeng Guo, Jiliang Tang, and Suhang Wang. 2023. A Comprehensive Survey on Trustworthy Graph Neural Networks: Privacy, Robustness, Fairness, and Explainability. *arXiv preprint arXiv:2204.08570* (2023).
- [12] Chenhui Deng, Zichao Yue, and Zhiru Zhang. 2024. Polynormer: Polynomial-expressive graph transformer in linear time. In *The 12th International Conference on Learning Representations*.
- [13] Yushun Dong, Ninghao Liu, Brian Jalaian, and Jundong Li. 2022. EDITS: Modeling and Mitigating Data Bias for Graph Neural Networks. In *Proceedings of the ACM Web Conference 2024*. 1259–1269.
- [14] Yushun Dong, Jing Ma, Song Wang, Chen Chen, and Jundong Li. 2023. Fairness in graph mining: A survey. *IEEE Transactions on Knowledge and Data Engineering* 35, 10 (2023), 10583–10602.
- [15] Cynthia Dwork, Moritz Hardt, Toniann Pitassi, Omer Reingold, and Richard S. Zemel. 2012. Fairness through Awareness. In *Proceedings of Innovations in Theoretical Computer Science*. 214–226.
- [16] Matt Fredrikson, Somesh Jha, and Thomas Ristenpart. 2015. Model Inversion Attacks that Exploit Confidence Information and Basic Countermeasures. In *Proceedings of the 22nd ACM SIGSAC Conference on Computer and Communications Security*. 1322–1333.
- [17] Alessio Gravina, Moshe Eliasof, Claudio Gallicchio, Davide Bacci, and Carolina-Bibiane Schonlieb. 2025. On Oversquashing in Graph Neural Networks Through the Lens of Dynamical Systems. In *Proceedings of the 39th Annual AAAI Conference on Artificial Intelligence*. 16906–16914.
- [18] Dongliang Guo, Zhixuan Chu, and Sheng Li. 2023. Fair Attribute Completion on Graph with Missing Attributes. In *The 11th International Conference on Learning Representations*.
- [19] Moritz Hardt, Eric Price, and Nati Srebro. 2016. Equality of Opportunity in Supervised Learning. In *Proceedings of the 30th International Conference on Neural Information Processing Systems*. 3323–3331.
- [20] Yeh I-cheng and Lien Che-hui. 2009. The Comparisons of Data Mining Techniques for the Predictive Accuracy of Probability of Default of Credit Card Clients. *Expert Systems with Applications* 36, 2 (2009), 2473–2480.
- [21] Zhimeng Jiang, Xiaotian Han, Chao Fan, Zirui Liu, Ali Mostafavi, and Xia Hu. 2024. Chasing Fairness in Graphs: A GNN Architecture Perspective. In *Proceedings of the AAAI Conference on Artificial Intelligence*. 21214–21222.
- [22] Kareem L Jordan and Tina L Freiburger. 2015. The effect of race/ethnicity on sentencing: Examining sentence type, jail length, and prison length. *Journal of Ethnicity in Criminal Justice* 13, 3 (2015), 179–196.
- [23] Diederik P Kingma and Jimmy Ba. 2015. Adam: A method for Stochastic Optimization. In *The 3rd International Conference on Learning Representations*.
- [24] Thomas N Kipf and Max Welling. 2017. Semi-Supervised Classification with Graph Convolutional Networks. In *The 5th International Conference on Learning Representations*.
- [25] Devin Kreuzer, Dominique Beaini, William L. Hamilton, Vincent Letourneau, and Prudencio Tossou. 2021. Rethinking Graph Transformers with Spectral Attention. In *Proceedings of the 35th International Conference on Neural Information Processing Systems*. 21618–21629.
- [26] Jure Leskovec and Julian McAuley. 2012. Learning to Discover Social Circles in Ego Networks. In *Proceedings of the 25th International Conference on Neural Information Processing Systems*. 539–547.
- [27] Zhiyun Li, Yushun Dong, Qiang Liu, and Jeffrey Xu Yu. 2024. Rethinking Fair Graph Neural Networks from Re-balancing. In *Proceedings of the 30th ACM SIGKDD Conference on Knowledge Discovery and Data Mining*. 1736–1745.
- [28] Zhenghong Lin, Yuze Wu, Jiawei Chen, and Shiping Wang. 2024. RViT: Robust Fusion Vision Transformer with Variational Hierarchical Denoising Process for Image Classification. *Guidance, Navigation and Control* 4, 03 (2024), 2441007.
- [29] Renqiang Luo, Huafei Huang, Ivan Lee, Chengpei Xu, Jianzhong Qi, and Feng Xia. 2025. FairGP: A Scalable and Fair Graph Transformer Using Graph Partitioning. In *Proceedings of the 39th Annual AAAI Conference on Artificial Intelligence*. 12319–12327.
- [30] Renqiang Luo, Huafei Huang, Shuo Yu, Zhuoyang Han, Estrid He, Xiuzhen Zhang, and Feng Xia. 2024. FUGNN: Harmonizing Fairness and Utility in Graph Neural Networks. In *Proceedings of the 30th ACM SIGKDD Conference on Knowledge Discovery and Data Mining*. 2072–2081.
- [31] Renqiang Luo, Huafei Huang, Shuo Yu, Xiuzhen Zhang, and Feng Xia. 2024. FairGT: A Fairness-aware Graph Transformer. In *Proceedings of the 32nd International Joint Conference on Artificial Intelligence*. 449–457.
- [32] Nisareh Mehrabi, Fred Morstatter, Nripsuta Saxena, Kristina Lerman, and Aram Galstyan. 2021. A Survey on Bias and Fairness in Machine Learning. *ACM Computing Surveys* 54, 6 (2021), 1–35.
- [33] Ahsan Shehzad, Feng Xia, Shagufta Abid, Ciyuan Peng, Shuo Yu, Dongyu Zhang, and Karin Verspoor. 2024. Graph Transformers: A Survey. *arXiv preprint arXiv:2407.09777* (2024).
- [34] Lubos Takac and Zabovsky Michal. 2012. Data Analysis in Public Social Networks. In *Proceedings of International Scientific Conference and International Workshop Present Day Trends of Innovations*.
- [35] Ashish Vaswani, Noam Shazeer, Niki Parmar, Jakob Uszkoreit, Llion Jones, Aidan N Gomez, Łukasz Kaiser, and Illia Polosukhin. 2017. Attention is All You Need. In *Proceedings of the 31st International Conference on Neural Information Processing Systems*. 6000–6010.
- [36] Huaiyu Wan, Yutao Zhang, Jing Zhang, and Jie Tang. 2019. AMiner: Search and Mining of Academic Social Networks. *Data Intelligence* 1, 1 (2019), 58–76.
- [37] Qitian Wu, Wentao Zhao, Chenxiao Yang, Hengrui Zhang, Fan Nie, Haitian Jiang, Yatao Bian, and Junchi Yan. 2023. SGFormer: Simplifying and Empowering Transformers for Large-Graph Representations. In *Proceedings of the 37th International Conference on Neural Information Processing Systems*.
- [38] Yuxia Wu, Yuan Fang, and Lizi Liao. 2024. On the Feasibility of Simple Transformer for Dynamic Graph Modeling. In *Proceedings of the ACM Web Conference 2024*. 870–880.
- [39] Zhanhao Wu, Paras Jain, Matthew A. Wright, Azalia Mirhoseini, Joseph E. Gonzalez, and Ion Stoica. 2021. Representing Long-range Context for Graph Neural Networks with Global Attention. In *Proceedings of the 35th International Conference on Neural Information Processing Systems*. 13266–13279.
- [40] Zhishang Xiang, Chuanjie Wu, Qinggang Zhang, Shengyuan Chen, Zijin Hong, Xiao Huang, and Jinsong Su. 2025. When to use graphs in rag: A comprehensive analysis for graph retrieval-augmented generation. *arXiv preprint arXiv:2506.05690* (2025).
- [41] Yujie Xing, Xiao Wang, Yibo Li, Hai Huang, and Chuan Shi. 2024. Less is More: On the Over-Globalizing Problem in Graph Transformers. In *Proceedings of the 41st International Conference on Machine Learning*. 54656–54672.
- [42] Cheng Yang, Jixi Liu, Yunhe Yan, and Chuan Shi. 2024. FairSIN: Achieving Fairness in Graph Neural Networks through Sensitive Information Neutralization. In *Proceedings of the AAAI Conference on Artificial Intelligence*. 9241–9249.
- [43] Qinggang Zhang, Shengyuan Chen, Yuanchen Bei, Zheng Yuan, Huachi Zhou, Zijin Hong, Hao Chen, Yilin Xiao, Chuang Zhou, Junnan Dong, et al. 2025. A survey of graph retrieval-augmented generation for customized large language models. *arXiv preprint arXiv:2501.13958* (2025).
- [44] Qinggang Zhang, Keyu Duan, Junnan Dong, Pai Zheng, and Xiao Huang. 2024. Logical reasoning with relation network for inductive knowledge graph completion. In *Proceedings of the 30th ACM SIGKDD Conference on Knowledge Discovery and Data Mining*. 4268–4277.
- [45] Yuchen Zhang, Xiaoxiao Ma, Jia Wu, Jian Yang, and Hao Fan. 2024. Heterogeneous Subgraph Transformer for Fake News Detection. In *Proceedings of the ACM Web Conference 2024*. 1272–1282.
- [46] Luying Zhong, Jielong Lu, Zhaoliang Chen, Na Song, and Shiping Wang. 2024. Adaptive Multi-channel Constrained Graph Convolutional Network with Graph adn Feature Fusion. *Information Sciences* 658 (2024), 120012.
- [47] Zijie Zhou, Zhaoqi Lu, Xuekai Wei, Rongqin Chen, Shenghui Zhang, Pak Lon Ip, and Leong Hou U. 2025. Tokenphormer: Structure-aware Multi-token Graph Transformer for Node Classification. In *Proceedings of the 39th Annual AAAI Conference on Artificial Intelligence*. 13428–13463.

A Ethical Use of Data and Informed Consent

All datasets used in this study (e.g., Credit, AMiner-S, and other benchmark social network datasets) are publicly available under their respective research licenses. These datasets were released for research purposes and have been widely adopted in prior work on graph learning and fairness-aware machine learning. They do not contain personally identifiable information beyond what has been made publicly accessible, and no additional data collection or annotation was conducted by the authors. As this work relies solely on secondary analysis of existing open datasets, no direct interaction with human participants occurred, and informed consent was not required. The study complies with the ethical use of data guidelines established by the research community.

B Theoretical Analysis and Proofs

Theorem 1: *The effect of utilising the principal eigenvector as a structural encoding, in comparison to using multiple adjacency matrices as structural topology encoding for multi-hop sensitive attributes under incomplete sensitive attributes, can be approximated. The following equation holds:*

$$\lim_{k \rightarrow \infty} \cos(\langle \mathbf{A}^k \mathbf{H}'[:, s], \mathbf{H}'[:, s] \rangle) = \cos(\langle \mathbf{p}_1, \mathbf{H}'[:, s] \rangle). \quad (17)$$

Proof. We assume $\gamma_i = \mathbf{H}'[:, s]^\top \mathbf{p}_i$. Since $\mathbf{A} \in \mathbb{R}^{n \times n}$ is a symmetric matrix, the eigendecomposition of \mathbf{A} can be written as $\mathbf{P} = (\mathbf{p}_1, \mathbf{p}_2, \dots, \mathbf{p}_n)$, and $\|\mathbf{p}_i\| = 1$ ($i \in \{1, 2, \dots, n\}$) and $\Lambda = \text{diag}(\lambda_1, \lambda_2, \dots, \lambda_n)$. Thus,

$$\begin{aligned} & \lim_{k \rightarrow \infty} \cos(\langle \mathbf{A}^k \mathbf{H}'[:, s], \mathbf{H}'[:, s] \rangle) \\ &= \lim_{l \rightarrow \infty} \frac{(\mathbf{A}^k \mathbf{H}'[:, s])^\top \mathbf{H}'[:, s]}{\|\mathbf{A}^k \mathbf{H}'[:, s]\| \|\mathbf{H}'[:, s]\|} \\ &= \lim_{l \rightarrow \infty} \frac{(\mathbf{A}^k \mathbf{H}'[:, s])^\top \mathbf{H}'[:, s]}{\sqrt{(\mathbf{A}^k \mathbf{H}'[:, s])^\top \mathbf{A}^k \mathbf{H}'[:, s]} \sqrt{\mathbf{H}'[:, s]^\top \mathbf{H}'[:, s]}}. \end{aligned}$$

Because,

$$\begin{aligned} \mathbf{A}^k \mathbf{H}'[:, s] &= \mathbf{P} \Lambda^k \mathbf{P}^\top \mathbf{H}'[:, s], \\ \gamma_i &= \mathbf{H}'[:, s]^\top \mathbf{p}_i. \end{aligned}$$

Thus,

$$\begin{aligned} & \lim_{k \rightarrow \infty} \cos(\langle \mathbf{A}^k \mathbf{H}'[:, s], \mathbf{H}'[:, s] \rangle) \\ &= \lim_{k \rightarrow \infty} \frac{\sum_{i=1}^n \gamma_i^2 \lambda_i^k}{\sqrt{\sum_{i=1}^n \gamma_i^2 \lambda_i^{2k}} \sqrt{\sum_{i=1}^n \gamma_i^2}} \\ &= \lim_{k \rightarrow \infty} \frac{\gamma_1^2 + \sum_{i=2}^n \gamma_i^2 (\frac{\lambda_i}{\lambda_1})^k}{\sqrt{\gamma_1^2 + \sum_{i=2}^n \gamma_i^2 (\frac{\lambda_i}{\lambda_1})^{2k}} \sqrt{\sum_{i=1}^n \gamma_i^2}} \\ &= \frac{\gamma_1}{\sqrt{\sum_{i=1}^n \gamma_i^2}}. \end{aligned}$$

Because,

$$\begin{aligned} \cos(\langle \mathbf{p}_1, \mathbf{H}'[:, s] \rangle) &= \frac{\mathbf{H}'[:, s]^\top \mathbf{p}_1}{\|\mathbf{H}'[:, s]\| \|\mathbf{p}_1\|} = \frac{\mathbf{H}'[:, s]^\top \mathbf{p}_1}{\|\mathbf{H}'[:, s]\|} \\ &= \frac{\mathbf{H}'[:, s]^\top \mathbf{p}_1}{\sqrt{\mathbf{H}'[:, s]^\top \mathbf{H}'[:, s]}} \\ &= \frac{\mathbf{H}'[:, s]^\top \mathbf{p}_1}{\sqrt{(\mathbf{P}^\top \mathbf{H}'[:, s])^\top \mathbf{P}^\top \mathbf{H}'[:, s]}} \\ &= \frac{\mathbf{H}'[:, s]^\top \mathbf{p}_1}{\sqrt{\sum_{j=1}^n (\mathbf{H}'[:, s]^\top \mathbf{p}_j)^2}} \\ &= \frac{\gamma_1}{\sqrt{\sum_{j=1}^n \gamma_j^2}}. \end{aligned}$$

Then,

$$\lim_{k \rightarrow \infty} \cos(\langle \mathbf{A}^k \mathbf{H}'[:, s], \mathbf{H}'[:, s] \rangle) = \cos(\langle \mathbf{p}_1, \mathbf{H}'[:, s] \rangle).$$

□

Theorem 1.1: *In cases where multiple maximal eigenvalues exist, the conclusions remain analogous, with further elaboration as following:*

$$\begin{aligned} & \lim_{l \rightarrow \infty} \cos(\langle \mathbf{A}^k \mathbf{H}'[:, s], \mathbf{H}'[:, s] \rangle) \\ & \geq \frac{1}{\sqrt{j}} \sum_{i=1}^j \cos(\langle \mathbf{H}'[:, s], \mathbf{p}_i \rangle). \end{aligned} \quad (18)$$

Proof.

$$\begin{aligned} & \lim_{k \rightarrow \infty} \cos(\langle \mathbf{A}^k \mathbf{H}'[:, s], \mathbf{H}'[:, s] \rangle) \\ &= \lim_{k \rightarrow \infty} \frac{\sum_{i=1}^n \gamma_i^2 \lambda_i^k}{\sqrt{\sum_{i=1}^n \gamma_i^2 \lambda_i^{2k}} \sqrt{\sum_{i=1}^n \gamma_i^2}} \\ &= \lim_{k \rightarrow \infty} \frac{\sum_{i=1}^j \gamma_i^2 + \sum_{i=j+1}^n \gamma_i^2 (\frac{\lambda_i}{\lambda_1})^k}{\sqrt{\sum_{i=1}^j \gamma_i^2 + \sum_{i=j+1}^n \gamma_i^2 (\frac{\lambda_i}{\lambda_1})^{2k}} \sqrt{\sum_{i=1}^n \gamma_i^2}} \\ &= \frac{\sqrt{\sum_{i=1}^j \gamma_i^2}}{\sqrt{\sum_{i=1}^n \gamma_i^2}}. \end{aligned}$$

Then, considering $\cos(\langle \mathbf{H}'[:, s], \mathbf{p}_i \rangle) = \frac{\gamma_i}{\sqrt{\sum_{i=1}^n \gamma_i^2}}$ and the Cauchy-Schwarz Inequality, we have:

$$\begin{aligned} & \lim_{l \rightarrow \infty} \cos(\langle \mathbf{A}^k \mathbf{H}'[:, s], \mathbf{H}'[:, s] \rangle) = \frac{1}{\sqrt{j}} \frac{\sqrt{j * 1^2 \sum_{i=1}^j \gamma_i^2}}{\sqrt{\sum_{i=1}^n \gamma_i^2}} \\ & \geq \frac{1}{\sqrt{j}} \frac{\sum_{i=1}^j \gamma_i}{\sqrt{\sum_{i=1}^n \gamma_i^2}} = \frac{1}{\sqrt{j}} \sum_{i=1}^j \cos(\langle \mathbf{H}'[:, s], \mathbf{p}_i \rangle). \end{aligned}$$

Especially, only if right-side terms $\cos(\langle \mathbf{H}'[:, s], \mathbf{p}_i \rangle)$ are equal, the equation holds.

□

Theorem 1.2 *The effect of non-principal eigenvalues diminishes at an exponential rate.*

Proof. Let $\mathbf{T}^k = \cos(\langle \mathbf{A}^k \mathbf{H}'[:, s], \mathbf{H}'[:, s] \rangle)$, thus:

$$\mathbf{T}^k = \frac{\gamma_1^2 + \sum_{i=2}^n \gamma_i^2 (\frac{\lambda_i}{\lambda_1})^k}{\sqrt{\gamma_1^2 + \sum_{i=2}^n \gamma_i^2 (\frac{\lambda_i}{\lambda_1})^{2k}} \cdot \sqrt{\sum_{i=1}^n \gamma_i^2}}.$$

Let $\frac{\gamma_i}{\gamma_1} = u_i, \frac{\lambda_i}{\lambda_1} = v_i < 1$, thus:

$$\mathbf{T}^k = \frac{1 + \sum_{i=2}^n u_i^2 v_i^k}{\sqrt{1 + \sum_{i=2}^n u_i^2 v_i^{2l}}} \sqrt{1 + \sum_{i=2}^n u_i^2}.$$

Let $\mathbf{T}' = \lim_{l \rightarrow \infty} \mathbf{T}^k$, thus:

$$\mathbf{T}' = \frac{\gamma_1}{\sqrt{\sum_{i=1}^n \gamma_i^2}} = \frac{1}{\sqrt{1 + \sum_{i=2}^n u_i^2}}.$$

Using the Taylor expansion of the multivariate function $f(\mathbf{x})$ (second order):

$$\begin{aligned} f(\mathbf{x}) &= f(\mathbf{x}_0) + \nabla f(\mathbf{x}_0)^\top (\mathbf{x} - \mathbf{x}_0) \\ &\quad + \frac{1}{2} (\mathbf{x} - \mathbf{x}_0)^\top \nabla^2 f(\mathbf{x}_0) (\mathbf{x} - \mathbf{x}_0) + o(\|\mathbf{x} - \mathbf{x}_0\|^2) \end{aligned}$$

Let $x_i = u_i v_i^k, f(x_2, \dots, x_n) = \sqrt{1 + \sum_{i=2}^n x_i^2}$. Thus,

$$\frac{\partial f}{\partial x_i} = \frac{1}{2} \cdot \frac{1 \cdot 2x_i}{\sqrt{1 + \sum_{i=2}^n x_i^2}} = \frac{x_i}{\sqrt{1 + \sum_{i=2}^n x_i^2}}.$$

When $x_2 = \dots = x_n = 0$,

$$\begin{aligned} \frac{\partial f}{\partial x_i} &= 0 \\ \frac{\partial f}{(\partial x_i)^2} &= \frac{\sqrt{1 + \sum_{i=2}^n x_i^2} \cdot 1 - x_i \cdot \left(-\frac{1}{2}\right) \cdot \frac{2x_i}{\sqrt{(1 + \sum_{i=2}^n x_i^2)^3}}}{1 + \sum_{i=2}^n x_i^2} \\ &= \frac{1}{\sqrt{1 + \sum_{i=2}^n x_i^2}} + \frac{x_i^2}{\sqrt{(1 + \sum_{i=2}^n x_i^2)^5}}. \end{aligned}$$

When $x_2 = \dots = x_n = 0$,

$$\begin{aligned} \frac{\partial f}{(\partial x_i)^2} &= 1. \\ \frac{\partial f}{\partial x_i \partial x_j} &= \frac{x_i x_j}{\sqrt{(1 + \sum_{i=2}^n x_i^2)^5}}. \end{aligned}$$

When $x_2 = \dots = x_n = 0$,

$$\frac{\partial f}{\partial x_i \partial x_j} = 0.$$

Thus, the Taylor expansion of $f(x_2, \dots, x_n)$ at $(0, \dots, 0)$:

$$\begin{aligned} f(x_2, \dots, x_n) &= f(0, \dots, 0) + \sum_{i=2}^n (x_i - 0) f' x_i (0, \dots, 0) \\ &\quad + \frac{1}{2} \sum_{i,j=2}^n (x_i - 0) (x_j - 0) f'' x_i x_j (0, \dots, 0) \\ &\quad + o^2 \\ &= 1 + 0 + \frac{1}{2} \sum_{i=2}^n x_i^2 + o^2 \\ &= 1 + \frac{1}{2} \sum_{i=2}^n x_i^2 + o^2. \end{aligned}$$

Thus:

$$\begin{aligned} \sqrt{1 + \sum_{i=2}^n (u_i v_i^k)^2} &= 1 + \frac{1}{2} \sum_{i=2}^n (u_i v_i^k)^2 + o^2, \\ \sqrt{1 + \sum_{i=2}^n (u_i v_i^{l+1})^2} &= 1 + \frac{1}{2} \sum_{i=2}^n (u_i v_i^{l+1})^2 + o^2. \end{aligned}$$

Because $\lim_{l \rightarrow \infty} \left(1 + \frac{1}{2} \sum_{i=2}^n (u_i v_i^k)^2\right) = 1$, thus

$$\begin{aligned} \lim_{l \rightarrow \infty} \frac{\mathbf{T}^{l+1} - \mathbf{T}'}{\mathbf{T}^k - \mathbf{T}'} &= \lim_{l \rightarrow \infty} \frac{\sum_{i=2}^n u_i^2 v_i^{l+1} - \sum_{i=2}^n \frac{1}{2} u_i^2 v_i^{2l+2}}{\sum_{i=2}^n u_i^2 v_i^k - \sum_{i=2}^n \frac{1}{2} u_i^2 v_i^{2l}} \\ &= \lim_{l \rightarrow \infty} \frac{\sum_{i=2}^n u_i^2 (v_i^{l+1} - \frac{1}{2} v_i^{2l+2})}{\sum_{i=2}^n u_i^2 (v_i^k - \frac{1}{2} v_i^{2l})} \\ &= \lim_{l \rightarrow \infty} \frac{\sum_{i=2}^n u_i^2 v_i^{l+1}}{\sum_{i=2}^n u_i^2 v_i^k} \\ &= \lim_{l \rightarrow \infty} \frac{u_2^2 v_2^{l+1} + \sum_{i=3}^n u_i v_i^{l+1}}{u_2^2 v_2^k + \sum_{i=3}^n u_i v_i^k}. \end{aligned}$$

Let $\frac{v_i}{v_2} = \omega_i < 1$, thus:

$$\begin{aligned} \lim_{l \rightarrow \infty} \frac{\mathbf{T}^{l+1} - \mathbf{T}'}{\mathbf{T}^k - \mathbf{T}'} &= \lim_{l \rightarrow \infty} \frac{u_2^2 v_2 \cdot v_2^k + \sum_{i=3}^n u_i \omega_i^k v_i \cdot v_2^k}{u_2^2 \cdot v_2^k + \sum_{i=3}^n u_i w_i^k \cdot v_2^k} \\ &= \lim_{l \rightarrow \infty} \frac{u_2^2 v_2 + \sum_{i=3}^n u_i w_i^k v_i}{u_2^2 + \sum_{i=3}^n u_i \omega_i^k} \\ &= v_2 \\ &= \frac{\lambda_2}{\lambda_1}. \end{aligned}$$

Therefore, $\cos(\langle \mathbf{A}^k \mathbf{H}'[:, s], \mathbf{H}'[:, s] \rangle)$ decays exponentially with the rate determined by $\frac{\lambda_2}{\lambda_1}$. \square

Theorem 2: When sensitive attributes are incomplete, utilizing principal eigenvectors as structural topology encoding can effectively replicate the results achieved by using the adjacency matrix when the sensitive attributes are complete. The following equation holds:

$$\lim_{k \rightarrow \infty} \cos(\langle \mathbf{A}^k \mathbf{H}[:, s], \mathbf{H}'[:, s] \rangle) = \cos(\langle \mathbf{p}_1, \mathbf{H}'[:, s] \rangle). \quad (19)$$

Proof. We also assume $\alpha_i = \mathbf{H}[:, s]^\top \mathbf{p}_i$ and $\gamma_i = \mathbf{H}'[:, s]^\top \mathbf{p}_i$. Thus,

$$\begin{aligned} &\lim_{k \rightarrow \infty} \cos(\langle \mathbf{A}^k \mathbf{H}[:, s], \mathbf{H}'[:, s] \rangle) \\ &= \lim_{k \rightarrow \infty} \frac{\sum_{i=1}^n \alpha_i \gamma_i \lambda_i^k}{\sqrt{\sum_{i=1}^n \alpha_i^2 \lambda_i^{2k}} \sqrt{\sum_{i=1}^n \gamma_i^2}} \\ &= \lim_{k \rightarrow \infty} \frac{\sum_{i=2}^n \alpha_i \gamma_i \left(\frac{\lambda_i}{\lambda_1}\right)^k + \alpha_1 \gamma_1}{\sqrt{\alpha_1^2 + \sum_{i=2}^n \alpha_i^2 \left(\frac{\lambda_i}{\lambda_1}\right)^{2k}} \sqrt{\sum_{i=1}^n \gamma_i^2}} \\ &= \frac{\gamma_1}{\sqrt{\sum_{i=1}^n \gamma_i^2}}. \end{aligned}$$

Because,

$$\cos(\langle \mathbf{p}_1, \mathbf{H}'[:, s] \rangle) = \frac{\gamma_1}{\sqrt{\sum_{i=1}^n \gamma_i^2}}.$$

Then,

$$\lim_{k \rightarrow \infty} \cos(\langle \mathbf{A}^k \mathbf{H}[:, s], \mathbf{H}'[:, s] \rangle) = \cos(\langle \mathbf{p}_1, \mathbf{H}'[:, s] \rangle).$$

□

Theorem 3: *Padding the incomplete value with zeros can effectively recover the neighbouring sensitive attribute information in the scenario where sensitive attributes are incomplete. The following equation holds:*

$$\begin{aligned} & \lim_{k \rightarrow \infty} \cos(\langle \mathbf{A}^k \mathbf{H}'[:, s](0), \mathbf{H}[:, s] \rangle) \\ &= \lim_{k \rightarrow \infty} \cos(\langle \mathbf{A}^k \mathbf{H}[:, s], \mathbf{H}[:, s] \rangle). \end{aligned} \quad (20)$$

Proof. We denote $\mathbf{H}'[:, s](0)$ as $\mathbf{H}'[:, s](0) = \mathbf{I}_{n,t} \mathbf{H}[:, s]$, where

$$\mathbf{I}_{n,t} = \begin{cases} 1, & i = j \text{ and } v_i[s] \text{ is complete,} \\ 0, & \text{else.} \end{cases}$$

We assume $\alpha_i = \mathbf{H}[:, s]^\top \mathbf{p}_i$ and $\beta_i = \mathbf{H}[:, s]^\top \mathbf{I}_{n,t} \mathbf{p}_i$. Thus,

$$\begin{aligned} & \|\mathbf{A}^k \mathbf{H}'[:, s](0)\|^\top \\ &= \sqrt{(\mathbf{A}^k \mathbf{H}'[:, s](0))^\top \mathbf{A}^k \mathbf{H}'[:, s](0)} \\ &= \sqrt{\mathbf{H}'[:, s](0)^\top \mathbf{A}^{2k} \mathbf{H}'[:, s](0)} \\ &= \sqrt{\mathbf{H}'[:, s](0)^\top \mathbf{P} \Lambda^{2k} \mathbf{P}^\top \mathbf{H}'[:, s](0)} \\ &= \sqrt{\sum_{i=1}^n \beta_i^2 \lambda_i^{2k}}. \\ \|\mathbf{H}[:, s]\| &= \sqrt{(\mathbf{H}[:, s])^\top \mathbf{H}[:, s]} = \sqrt{\sum_{i=1}^n \alpha_i^2}. \end{aligned}$$

Therefore,

$$\begin{aligned} & \lim_{k \rightarrow \infty} \cos(\langle \mathbf{A}^k \mathbf{H}'[:, s](0), \mathbf{H}[:, s] \rangle) \\ &= \lim_{k \rightarrow \infty} \frac{(\mathbf{A}^k \mathbf{H}'[:, s](0))^\top \mathbf{H}[:, s]}{\|\mathbf{A}^k \mathbf{H}'[:, s](0)\|^\top \|\mathbf{H}[:, s]\|} \\ &= \lim_{k \rightarrow \infty} \frac{\mathbf{H}'[:, s]^\top (\mathbf{I}_{n,t} \mathbf{P} \Lambda^{2k} \mathbf{P}^\top) \mathbf{H}[:, s]}{\|\mathbf{A}^k \mathbf{H}'[:, s](0)\|^\top \|\mathbf{H}[:, s]\|} \\ &= \lim_{k \rightarrow \infty} \frac{\sum_{i=1}^n \alpha_i \beta_i \lambda_i^k}{\sqrt{\sum_{i=1}^n \beta_i^2 \lambda_i^{2k}} \sqrt{\sum_{i=1}^n \alpha_i^2}}. \end{aligned}$$

Because $\lambda_1 \gg \lambda_i$:

$$\begin{aligned} & \lim_{k \rightarrow \infty} \cos(\langle \mathbf{A}^k \mathbf{H}'[:, s](0), \mathbf{H}[:, s] \rangle) \\ &= \lim_{k \rightarrow \infty} \frac{\alpha_1 \beta_1 + \sum_{i=2}^n \alpha_i \beta_i (\frac{\lambda_i}{\lambda_1})^k}{\sqrt{\beta_1^2 + \sum_{i=2}^n \beta_i^2 (\frac{\lambda_i}{\lambda_1})^{2k}} \sqrt{\sum_{i=1}^n \alpha_i^2}} \\ &= \lim_{k \rightarrow \infty} \frac{\alpha_1 \beta_1}{\sqrt{\beta_1^2} \sqrt{\sum_{i=1}^n \alpha_i^2}} \\ &= \frac{\alpha_1}{\sqrt{\sum_{i=1}^n \alpha_i^2}} \\ &= \lim_{k \rightarrow \infty} \cos(\langle \mathbf{A}^k \mathbf{H}[:, s], \mathbf{H}[:, s] \rangle). \end{aligned}$$

C Experimental Setting

All experiments are conducted on Ubuntu with 128GB RAM and dual NVIDIA V100 GPUs (16GB each). The implementation is based on PyTorch 1.13.1 and PyTorch-Geometric 2.5.3. Model training uses the Adam optimizer [23] with 300 epochs, a learning rate of 0.01, and weight decay of $5e-4$. Hidden dimensions are varied across {16, 32, 64, 128} for comprehensive evaluation. To test robustness under incomplete data, attribute missing rates are set to six levels: {0.1, 0.2, 0.3, 0.4, 0.5, 0.6}. Model performance is assessed using accuracy for predictive capability, along with statistical parity and equality opportunity for fairness evaluation.